

Gas and Water Vapor Transport through a Series of Novel Poly(aryl ether sulfone) Membranes

Zhonggang Wang,^{*,†} Tianlu Chen,[‡] and Jiping Xu[‡]

Institute of Chemistry, Chinese Academy of Sciences, Beijing, 100080, P. R. China, and Changchun Institute of Applied Chemistry, Chinese Academy of Sciences, Changchun, 130022, P. R. China

Received July 9, 2001

ABSTRACT: The permeation behavior of water vapor, H₂, CO₂, O₂, N₂, and CH₄ gases in a series of novel poly(aryl ether sulfone)s has been examined over a temperature range of 30–100 °C. These polymers include four alkyl-substituted cardo poly(aryl ether sulfone)s and four intermolecular interaction enhanced poly(aryl ether sulfone)s. Their water vapor and gas transport properties were compared to the unmodified cardo poly(aryl ether sulfone) (PES-C). It was found that the bulky alkyl substituents on the phenylene rings were advantageous for gas permeability, while the intermolecular hydrogen bonds and ionic bonds resulted in a considerable increase in gas permselectivity. The causes of the trend were interpreted according to free volume, interchain distance, and glass transition temperature, together with the respective contribution of gas solubility and diffusivity to the overall permeability. Of interest was the observation that IMPES-L, which simultaneously bears bulky isopropyl substituent and pendant carboxylic groups, displayed 377% higher O₂ permeability and 5.3% higher O₂/N₂ permselectivity than PES-C. Furthermore, sodium salt form PES–Na⁺ and potassium salt form PES–K⁺ exhibited water vapor permeability twice as high as PES-C and H₂O/N₂ selectivity in 10⁵ order of magnitude.

Introduction

Over the past decade, a great deal of interest has been focused on the development of new high-performance polymeric membrane materials with high permeability and permselectivity for the specific gas separation requirements, including hydrogen recovery from reactor purge gas, nitrogen and oxygen enrichment, and stripping of carbon dioxide from natural gas as well as water vapor removal from air, etc.^{1,2} In this regard, it is very important to investigate the relationship between structure and gas transport properties.

In stiff-chain glassy polymers, recent studies indicate that the gas permeation behavior is mainly affected by the packing density and the segmental motion of the polymer chain. The high permeability is primarily caused by high free volume, while significant increase in gas permselectivity may be due to restricted segmental motion.^{3–6} On the basis of these facts, one can design new polymer to combine the two favorable factors, thus preparing polymers with both high gas permeability and high permselectivity.

A review of gas permeability literature revealed that, relative to the numerous papers on the polymer gas transport properties at room temperature, studies on high-temperature gas separation are rather rare. However, from the viewpoint of energy saving, in some cases, e.g. “C₁ chemistry”, it is desirable for the membrane separation process to be operated at the highest allowable temperature, so that the purge streams from synthesis gas production can be regulated in composition and recycled without extensive cooling and reheating prior to recycling to the reactor. Therefore, the effect of temperature on gas permeability is of great impor-

tance for membrane separation applications at high temperature.

Phenolphthalein-based cardo poly(aryl ether sulfone) (PES-C) has been noted for its excellent mechanical toughness, thermooxidative stability, and high glass transition temperature. Moreover, PES-C is soluble in a few polar solvents such as DMF, NMP, and chloroform, so it can be easily cast into flexible tough film.⁷ The experimental results on its gas permeability studies revealed that, in comparison with conventional glassy polymers, such as bisphenol A polysulfone,⁸ bisphenol A polycarbonate,⁹ and polyimide (Kapton),¹⁰ the PES-C membrane possesses better gas transport properties,¹¹ but from the viewpoint of future practical application, its gas selectivity and permeability coefficient must be further improved.

The present paper mainly concerns the gas permeability of a series of new poly(aryl ether sulfone) membranes over a temperature range from 30 to 100 °C. Their permeability and selectivity of water vapor over nitrogen are also reported here. The systematic variations in chemical structure were expected to result in interesting and unique variations in physical properties, e.g., packing density and segmental motion of the polymer chain, which would significantly affect the gas and water vapor permeation behavior in polymer membranes. The effects of pendant alkyl substituents and carboxylic groups on the transport properties were explained according to wide-angle X-ray diffraction, differential scanning calorimetry, and free volume.

Experimental Section

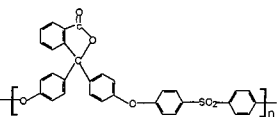
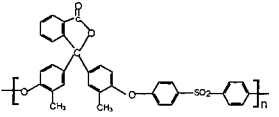
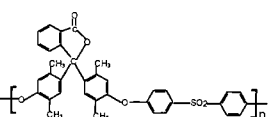
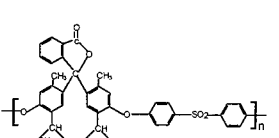
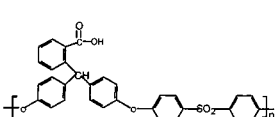
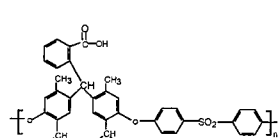
Materials. Phenolphthalein (PPH) and 2',2''-dimethylphenolphthalein (DMPPH) were purchased from Beijing Chemical Works and purified by recrystallization from a 50:50 (v/v) mixture of ethanol and water. Melting points are 262–263 and 220–222 °C, respectively. 2',2'',5',5''-Tetramethylphenolphthalein (TMPPH) and 2',2''-diisopropyl-5',5''-dimethylphenolphthalein (IMPPH) were purchased from Fluka Chemical Corp., with melting points of 239–240 and 251–252 °C, respectively, and were used as received. Bis(4-fluorophenyl) sulfone (DFDPS) was purchased from Aldrich Corp. and used

* To whom all correspondence should be addressed. Fax 0086-10-62559373; E-mail wangzhonggang@hotmail.com. Present address: Institute of Polymer Research Dresden e.V., Hohe Str. 6, 01069 Dresden, Germany.

[†] Institute of Chemistry.

[‡] Changchun Institute of Applied Chemistry.

Table 1. Chemical Structures of the Six Poly(aryl ether sulfone)s

Chemical Structure	Abbreviation	$\eta_{\text{RV}}(\text{dl/g})$	$\rho(\text{g/cm}^3)$
	PES-C	0.663	1.307
	DMPES-C	0.625	1.291
	TMPES-C	0.695	1.230
	IMPES-C	0.518	1.172
	PES-L	0.717	1.314
	IMPES-L	0.593	1.170

as received, dimethyl sulfoxide (DMSO) and *N,N*-dimethylformamide (DMF) were purified by vacuum distillation just before use, anhydrous potassium carbonate was finely powdered prior to use, and phenolphthalin (PPL) and 2',2''-diisopropyl-5',5''-dimethylphenolphthalin (IMPPL) were prepared in our laboratory according to the references.¹²

All the poly(aryl ether sulfone)s studied here were prepared via nucleophilic polycondensation from various bisphenols and DFDPS in DMSO using K_2CO_3 as catalyst in a similar procedure to that described in paper.¹³ Their chemical structures as well as reduced viscosity and density data are presented in Table 1.

To obtain Na^+ -type and K^+ -type ionomers, PES-L and IMPES-L were first grounded into powder, and then they were soaked with an aqueous solution of sodium hydroxide or potassium hydroxide. After equilibrating the polymer with the solution for about 24 h, the solids were rinsed with distilled water to remove the excess electrolytes and then dried.

Thin Film Preparations. The polymer samples, except PES- Na^+ and PES- K^+ , were dissolved in DMF at a concentration of 8 wt %. The solution were cast onto a clean glass plate at 60 °C in an oven for 8 h, and then the films were transferred to a vacuum oven and dried further at 200 °C and 10 mmHg for 48 h. For PES- Na^+ and PES- K^+ , the samples were dissolved in DMSO to form a solution of 10 wt %. The solutions were cast onto glass plate and dried at 100 °C for 10 h and then at 200 °C and 10 mmHg in a vacuum oven for additional 48 h. Films thickness were 35–40 μm .

Measurements. Reduced viscosities were measured using a Ubbelohde viscometer at a concentration of 0.5% (w/v) in DMF at 25 ± 0.01 °C.

Polymer densities were determined in a density gradient column containing aqueous solution of calcium nitrate at 30 °C.

Glass transition temperatures (T_g) were determined on a Perkin-Elmer DSC-7, over a temperature interval of 100–400

°C at a heating rate of 20 °C/min. The T_g 's were read at the middle of the change in the heat capacity.

Free volume (V_F) of each polymer is given by the following equation:

$$V_F = V - V_0 \quad (1)$$

where V is specific volume, which can be calculated from the polymer density; V_0 is the occupied volume of the polymer at 0 K, which was calculated according to the group contribution method of Sugden.¹⁴

Wide-angle X-ray diffraction (WAXD) measurements were performed at room temperature on a D/Max-B X-ray diffractometer using Cu K α radiation at a wavelength of 1.54 Å (40 kV, 15 mA). The scanning rate was 2°/min over a range of $2\theta = 5$ –40°. The mean interchain distance or d spacing can be calculated with Bragg's equation:

$$\lambda = 2d \sin \theta \quad (2)$$

where θ refers to the angle of the peak maxima.

Pure gas permeability coefficients over the temperature interval from 30 to 100 °C for H_2 , O_2 , N_2 , CO_2 , and CH_4 were measured using an apparatus described in the literature.¹⁵ The permeation cell temperature was controlled within ± 0.2 °C, measured by a calibrated Cu–constantan thermocouple inserted just above the membrane. The feed pressure was 5 ± 0.05 atm, and the permeate side pressure was less than 1 mmHg and considered negligible. To eliminate the CO_2 plasticization effect, the permeability coefficient of CO_2 was measured after the other gases. All the gases used here were at least 99.99% in purity. The permeability coefficient (P) was obtained from the slope of pressure–time plots after steady state has been reached. The true diffusion coefficient (D) can be calculated from independent permeation and solubility experiments. For cases where independent solubility data are unavailable, an apparent diffusion coefficients (D_{app}) can be estimated from membrane thickness (l) and the time lag (θ) from the transient permeation measurement according to the relation^{16,17}

$$D_{\text{app}} = l^2/6\theta \quad (3)$$

The solubility coefficients (S) were calculated from $S = P/D$. The ideal separation factor ($\alpha_{A/B}$) of gas A relative to gas B was given by the relation

$$\alpha_{A/B} = P_A/P_B = (D_A/D_B)(S_A/S_B) \quad (4)$$

where P_A and P_B are the permeability coefficients for gases A and B, D_A and D_B are diffusivity coefficients, and S_A and S_B are solubility coefficients. The ratios D_A/D_B and S_A/S_B are known as the diffusivity selectivity and the solubility selectivity, respectively.

Permeabilities of water vapor (P_w) were measured at 30 °C using the cup method described in the previous report.¹⁸

$$P_w = qltA\Delta p \quad (5)$$

where q/t is the mean value of cup weight loss rate in g/s, l is the membrane thickness in cm, A is the area of membrane sample in cm^2 , and Δp is the transmembrane water vapor pressure difference in cmHg, which is equal to $s(R_1 - R_2)$, where s is the saturation pressure of water vapor at the test temperature in cmHg and R_1 and R_2 are the relative humidity of the upstream and downstream sides of the membrane, respectively.

Results and Discussion

Polymer Structural Characteristics. The first four polymers in Table 1 contain pendant cardo lactone group, differing only in the position, number, and kind of alkyl substituents on the phenylene ring. DMPES-C, TMPES-C, and IMPES-C are referred to 2',2''-

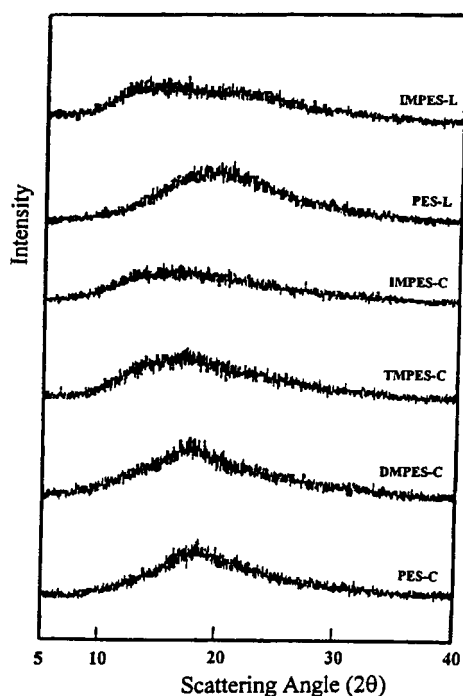


Figure 1. WAXD patterns of the polymer membranes.

dimethyl-substituted PES-C, 2',2'',5',5''-tetramethyl-substituted PES-C, and 2',2''-diisopropyl-5',5''-dimethyl-substituted PES-C, respectively. DMPES-C and IMPES-C displayed decreased T_g compared to that of PES-C due to the fact that the existence of substituents forced polymer chain apart from another, and the wider chain spacing was favorable for the polymer chain motion. However, tetramethyl-substituted TMPES-C showed an increased T_g by 13 °C. The reason that TMPES-C possesses higher T_g is not completely clear. A similar phenomenon had also been found from the tetramethyl-substituted bisphenol A polysulfone by Koros and Paul, who attributed the reason to that the symmetric substitution resulted in a larger chain stiffening effect than the asymmetric one.¹⁹

Through the chemical modification method, two carboxylic group-containing poly(aryl ether sulfone)s PES-L and IMPES-L were obtained by opening the lactonic ring of PES-C and IMPES-C. The enhanced polymer interchain interaction because of the hydrogen bonds between carboxylic groups on the backbone resulted in

PES-L and IMPES-L higher T_g than PES-C and IMPES-C, respectively.

After the ion exchange of H^+ with Na^+ or K^+ , two ionomers PES- Na^+ and PES- K^+ were obtained. The pendant carboxylate ions (COO^-) in ionomers can chelate not only with transitional metal ions (such as Al^{3+} , Fe^{3+}) but also with alkali metal ions (such as Na^+ or K^+), which has been confirmed in the literature.^{20,21} The chelation is very obvious for this series of polymers in this study. For example, PES-L could easily dissolve in DMSO, DMF, DMAc, and NMP, whereas PES- Na^+ and PES- K^+ were only soluble in DMSO on heating. Moreover, no glass transition was observed in a temperature interval of 100–400 °C, indicating that the ionic bonds between the carboxylate groups are so strong that the glass transition should take place at a temperature beyond 400 °C.

Interchain distance (d spacing) or free volume (V_F) can be used as a measure of the chain packing density or the "tightness" of polymer structure. Wide-angle X-ray diffractograms of six polymers are illustrated in Figure 1. All of the polymers are amorphous nature due to the presence of bulky pendant groups. It was observed that, relative to PES-C, the diffraction halos of substituted polymers shifted obviously toward smaller diffraction angle (2θ) with the increase of number and size of alkyl substituents. The d spacings of DMPES-C, TMPES-C, and IMPES-C, calculated from the eq 2, were 1.0%, 13.3%, and 25.5% larger than that of PES-C, respectively. As expected, the d spacing of PES-L was 2.1% smaller than that of PES-C due to the effect of interchain hydrogen bonds. However, despite the existence of carboxylic group, the d spacing of IMPES-L was 7.8% bigger than that of IMPES-C. The changing trend of free volume data in Table 2 was found to be consistent with that of d spacings except DMPES-C, which exhibited 5.2% lower free volume than PES-C. The possible reason is that the methyl groups on the phenylene ring can play two opposite roles on the polymer packing density. One is to open up the polymer chains, and this is favorable for the free volume. On the other hand, the relatively small methyl group may occupy the space between polymer chains. For DMPES-C, the latter effect is more evident, leading to its decreased free volume.

Gas Permeability, Diffusivity, and Solubility.

The gas permeability and selectivity coefficients for H_2 , O_2 , N_2 , CO_2 , and CH_4 at 30 °C are summarized in Tables 3 and 4. The permeability of H_2 , having the smallest

Table 2. Physical Properties of Polymers

polymers	T_g (°C)	$V_{30\text{ °C}}$ (cm ³ /g)	V_0 (cm ³ /g)	V_F (cm ³ /g)	$1/V_F$ (g/cm ³)	d spacing (Å)
PES-C	256	0.765	0.650	0.115	8.69	4.97
DMPES-C	245	0.775	0.666	0.109	9.17	5.02
TMPES-C	269	0.813	0.684	0.129	7.75	5.63
IMPES-C	230	0.853	0.691	0.162	6.17	6.24
IMPES-L	240	0.855	0.712	0.173	5.78	6.73
PES-L	262	0.761	0.669	0.092	10.8	4.78

Table 3. Gas Transport Properties of Polymers at 30 °C²²

polymers	P (barrers) ^a					α		
	H_2	O_2	N_2	CO_2	CH_4	H_2/N_2	O_2/N_2	CO_2/CH_4
PES-C	12.1	0.949	0.167	5.74	0.143	72.6	5.68	40.1
DMPES-C	10.8	0.868	0.110	3.12	0.0727	98.1	7.62	42.9
TMPES-C	16.9	1.55	0.201	7.69	0.225	84.1	8.46	34.2
IMPES-C	30.6	4.85	0.699	19.4	0.928	43.8	5.49	20.9
IMPES-L	49.6	4.53	0.757	25.1	1.13	65.5	5.98	22.3
PES-L	7.22	0.441	0.0437	2.25	0.0395	165	9.24	57.0

^a P in barrers; 1 barrer = 10^{-10} cm³ (STP) cm/(cm² s cmHg).

Table 4. Gas Transport Properties for PES-L Ionomer Series²²

polymers	<i>P</i> (barrers)			α	
	H ₂	O ₂	N ₂	H ₂ /N ₂	O ₂ /N ₂
PES-L	7.22	0.441	0.0437	165	9.24
PES-Na ⁺	5.05	0.281	0.0263	242	10.7
PES-K ⁺	4.89	0.208	0.0182	269	11.4

^a *P* in barrers; 1 barrer = 10⁻¹⁰ cm³ (STP) cm/(cm² s cmHg).

Table 5. Gas Physical Properties^{23–24}

gases	H ₂	CO ₂	O ₂	N ₂	CH ₄
<i>d</i> (Å)	2.80	3.30	3.46	3.64	3.80
<i>T_c</i> (K)	33.2	304.2	154.6	126.2	190.6

Table 6. Gas Diffusivities and Diffusivity Selectivities at 30 °C for Six Polymers

polymers	<i>D</i> (10 ⁻⁸ cm ² /s)				<i>D</i> _{O₂} / <i>D</i> _{N₂}	<i>D</i> _{CO₂} / <i>D</i> _{CH₄}
	O ₂	N ₂	CO ₂	CH ₄		
PES-C	3.24	0.685	1.23	0.132	4.73	9.31
DMPE-C	2.51	0.401	0.655	0.0648	6.26	10.1
TMPE-C	5.82	0.972	1.58	0.171	5.99	9.24
IMPE-C	12.3	2.62	3.64	0.593	4.67	6.14
IMPE-L	12.1	2.87	3.82	0.757	4.22	5.05
PES-L	1.35	0.184	0.352	0.0409	7.33	8.60

Table 7. Gas Solubilities and Solubility Selectivities at 30 °C

polymers	<i>S</i> (cm ³ (STP)/(cm ³ atm))				<i>S</i> _{O₂} / <i>S</i> _{N₂}	<i>S</i> _{CO₂} / <i>S</i> _{CH₄}
	O ₂	N ₂	CO ₂	CH ₄		
PES-C	0.220	0.185	3.55	0.824	1.19	4.31
DMPE-C	0.197	0.159	3.62	0.852	1.24	4.24
TMPE-C	0.222	0.157	3.69	1.02	1.41	3.69
IMPE-C	0.238	0.202	4.05	1.19	1.18	3.40
IMPE-L	0.285	0.201	4.99	1.13	1.41	4.42
PES-L	0.248	0.181	4.86	0.733	1.37	6.63

kinetic diameter (*d*) (see Table 5), is the highest and is followed by those of the progressively bigger penetrants except for IMPES-C and IMPES-L, in which CH₄ had higher permeability than N₂. The reason was thought to be due to the affinity effect between CH₄ molecule and bulky alkyl substituents, supported by the fact that IMPES-C and IMPES-L had a significantly high CH₄ solubility coefficient (see Table 7). The smaller free volume allowed DMPE-C and PES-L to reduce the gas permeability, especially the larger gas molecules such as nitrogen and methane decreased faster than the smaller one. As a result, DMPE-C and PES-L exhibited high gas permselectivity. For example, the selectivities of H₂/N₂ and O₂/N₂ in PES-L were 127% and 62.7% higher than that in PES-C, respectively. The bulky isopropyl and methyl substituents were highly effective in reducing the packing density of polymer chain and so as to extremely increase gas permeability. Compared to PES-L, the permeabilities of H₂, O₂, and CO₂ in IMPES-L increased by a factor of 7–11, and the permeabilities of N₂ and CH₄ increased by a factor of 17–29.

The enhanced interchain interaction was found to be very favorable for the increase of gas permselectivity. As shown in Table 4, PES-L, PES-Na⁺, and PES-K⁺, which had strong intermolecular hydrogen bonds or ionic bonds, displayed O₂/N₂ selectivity coefficient in 10.1, 10.7, and 11.4, respectively, and, to our knowledge, which were among the highest permselectivities reported previously in the literature.

Table 8. Diffusivity and Solubility Coefficients for PES-L Ionomer Series

polymers	<i>D</i> (10 ⁻⁸ cm ² /s)		<i>S</i> (cm ³ (STP)/(cm ³ atm))		<i>D</i> _{O₂} / <i>D</i> _{N₂}	<i>S</i> _{O₂} / <i>S</i> _{N₂}
	O ₂	N ₂	O ₂	N ₂		
PES-L	1.35	0.184	0.248	0.181	7.33	1.37
PES-Na ⁺	0.802	0.0946	0.247	0.195	8.48	1.27
PES-K ⁺	0.316	0.0349	0.501	0.396	9.05	1.46

In gas separation application, a tradeoff generally exists between permeability and permselectivity so that any improvement in permeability tends to be accompanied by a decrease in permselectivity, and vice versa. However, some results in this series of polymers were found to run counter to the above rule. Compared with PES-C, the O₂ permeabilities of TMPE-C and IMPES-L increased by 63% and 377%, respectively, and the O₂/N₂ selectivity coefficients of TMPE-C and IMPES-L also increased by 48.9% and 5.3%, respectively, exhibiting potential use as membrane material in O₂/N₂ separation application.

The results of gas diffusivity and diffusivity selectivity as well as gas solubility and solubility selectivity in the eight polymers are listed in Tables 6–8, where the diffusivity coefficients were obtained from the time-lag method, and the solubility coefficients were calculated by dividing the overall permeabilities by the diffusivity coefficients.

According to the “solution-diffusion” mechanism,²⁵ gas permeability depends on both the gas diffusivity and solubility. However, the extent of respective contribution of diffusivity and solubility factors on the permeability changed greatly from one gas pair to another. For the uncondensable O₂/N₂ gas pair, which had no obvious interaction between gases and polymer chains, the variations on gas diffusivity selectivities through the eight polymers were from 4.22 to 9.05, whereas solubility selectivities were only about 1.3. The gas diffusivities ranked in the order PES-K⁺ < PES-Na⁺ < PES-L < DMPE-L < PES-C < TMPE-C < IMPES-C < IMPES-L, which was the same as that of gas permeabilities. Therefore, the O₂/N₂ permeability and permselectivity were mainly determined by the variations in gas diffusivities, as in the case of most glassy polymer membrane materials.^{26,27} TMPE-C had the larger free volume and higher glass transition temperature; as a result, its O₂ diffusivity coefficient was 79.6% higher than that of PES-C, and its O₂/N₂ diffusivity selectivity coefficient also increased by 26.6%. This is why the O₂ permeability and O₂/N₂ permselectivity in TMPE-C simultaneously increased compared to that of PES-C.

Whereas for the CO₂/CH₄ gas pair, CO₂ displayed an obviously higher solubility coefficient because of its high critical temperature (see Table 5). For example, the gas diffusivity selectivities through the eight polymers were from 5.05 to 10.1, and the solubility selectivities were from 3.69 to 6.63. Therefore, relative to the O₂/N₂ gas pair, the solubility and solubility selectivity factors played a significantly increased part in the CO₂/CH₄ gas separation application.

The strengthened interchain interaction seriously inhibited the diffusivities of gas molecules, especially the gas molecules with larger kinetic diameters. Therefore, the ion-containing polymers exhibited extremely high gas permselectivity. For example, the permselectivity of H₂/N₂ in PES-K⁺ is 63% higher than that of PES-L and 271% higher than that of PES-C.

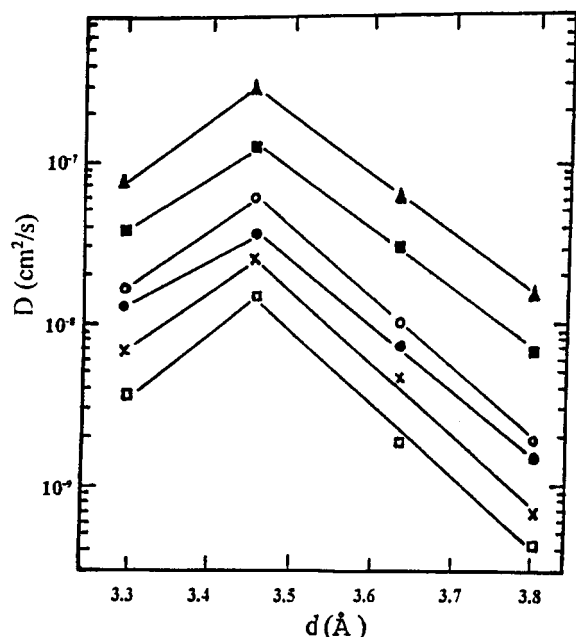


Figure 2. Plots of $\log D$ vs penetrant size (d) for these polymers: (□) PES-L; (×) DMPES-C; (●) PES-C; (○) TMPES-C; (■) IMPES-C; (▲) IMPES-L $\times 2$.

The relationships between gas diffusivity coefficients ($\log D$) and gas molecular kinetic diameters (d) were given in Figure 2. For O_2 , N_2 , and CH_4 , which had a similar critical temperature, a straight line was obtained, and the gas diffusivities decreased with the increase of penetrant size. However, for CO_2 , despite the smaller molecule size, its diffusivity coefficient was measured to be far lower than that of O_2 , which can be attributed to the energetically favorable interaction of CO_2 with the large number of polar groups in the polymer, and these polar groups act to impede its diffusivity.^{28,29}

Previous reports had shown that the gas diffusivity coefficients for a given gas in different polymers could be correlated well with the free volumes of the polymers according to the following relation:^{30–32}

$$D = Ae^{-B/VF} \quad (6)$$

in which the parameters A and B depend on the type of gases.

As seen in Figure 3, a fairly good correlation of O_2 diffusivity with free volumes of the six polymers was achieved; i.e., the polymer with more free volume generally had higher diffusivity coefficients. The deviation from the expected values based on above equation can be associated with the structure of the pendant group and its specific characteristics.

Temperature Dependence. In the temperature range 30–100 °C, the relationships between gas permeability and diffusivity with temperature for all the polymers studied here were consistent well with Arrhenius equations:

$$P = P_0 e^{-E_p/RT} \quad (7)$$

$$D = D_0 e^{-E_D/RT} \quad (8)$$

where P_0 and D_0 are preexponential factors, R is the gas constant, and E_p and E_D are the apparent activation energy of gas permeation and diffusion.

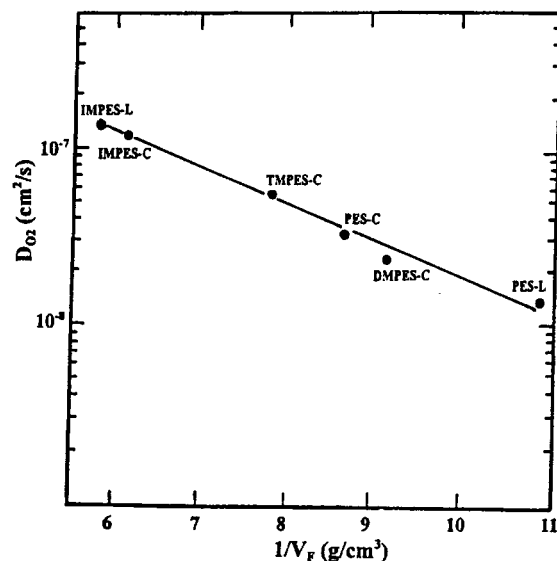


Figure 3. Correlation between O_2 diffusivity coefficients and free volume of polymers.

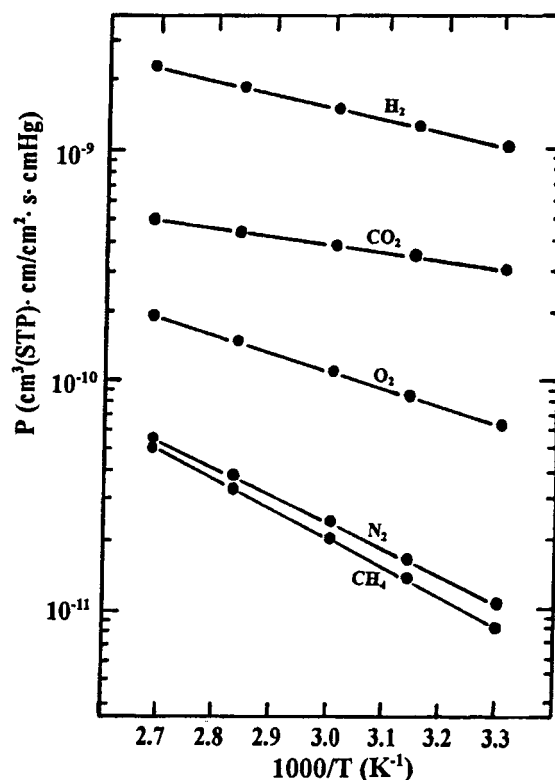


Figure 4. Plots of gas permeability as a function of reciprocal of temperature in DMPES-C.

Typical curves of $\log P$ vs $1/T$ and $\log D$ vs $1/T$ for DMPES-C and IMPES-L are given in Figures 4–7. The E_p s and E_D s for the five gases were calculated from the slope of Arrhenius plots. The heats of solution were obtained by the equation $H_s = E_p - E_D$. As shown in Tables 9–11, for the five gases, E_p s were on the order of $CH_4 > N_2 > O_2 > H_2 > CO_2$. Among the five gases, CH_4 exhibited the highest permeation activation energy, whereas the lowest E_p of CO_2 was due to its low heat of solution. The E_p s and E_D s in this series of polymers were listed in the same order of $PES-K^+ > PES-Na^+ > PES-L > DMPES-C > TMPES-C > IMPES-C > IMPES-L$, which was inversely related to the free volumes.

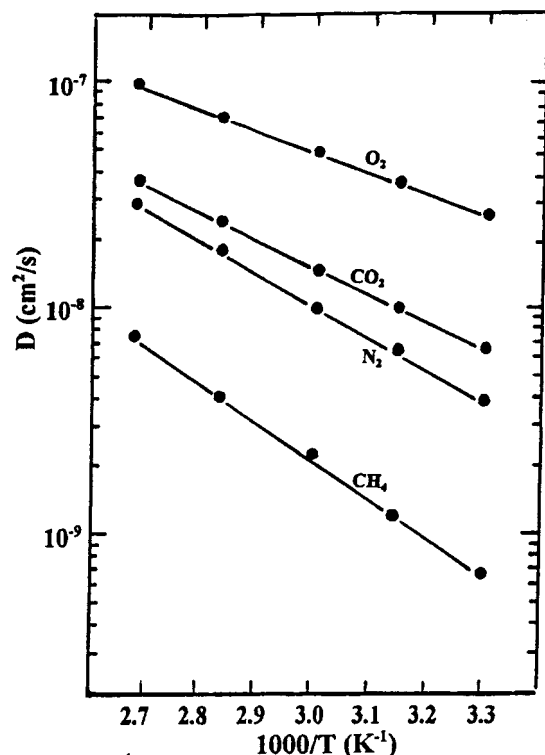


Figure 5. Plots of gas diffusivity as a function of reciprocal of temperature in DMPES-C.

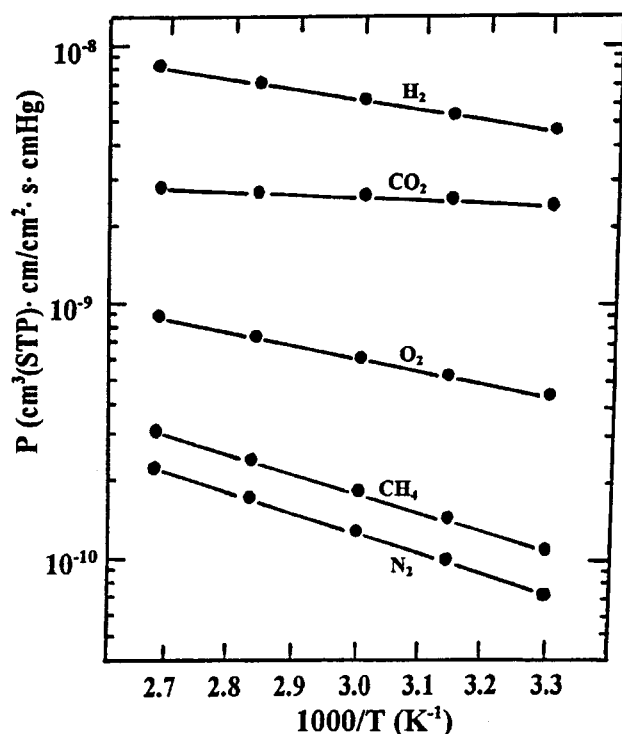


Figure 6. Plots of gas permeability as a function of reciprocal of temperature in IMPES-L.

According to Meares's gas diffusion hypothesis,³³ E_D was equated to the product of cohesive energy density (CED) and the volume of the diffusional cylinder:

$$E_D = (\pi/4)\delta^2\lambda(\text{CED}) \quad (9)$$

where δ is the diameter of the cylinder and λ is the diffusional length. The term $(\pi/4)\delta^2\lambda$ is the required

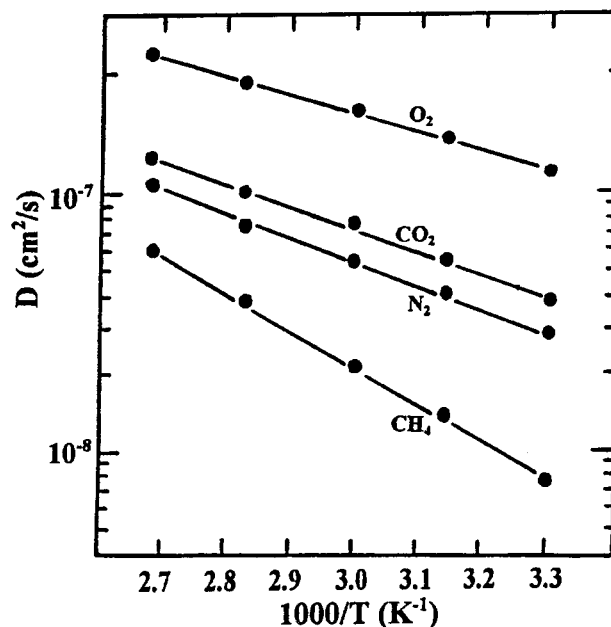


Figure 7. Plots of gas diffusivity as a function of reciprocal of temperature in IMPES-L.

Table 9. Apparent Permeation Activation Energies

polymers	E_p (kJ/mol)				
	H ₂	O ₂	N ₂	CO ₂	CH ₄
PES-C	10.9	12.5	18.6	8.07	21.4
DMPES-C	11.3	15.1	23.4	8.49	24.8
TMPES-C	10.2	9.42	14.6	4.12	15.6
IMPES-C	8.19	8.23	12.6	2.18	12.4
IMPES-L	7.69	9.16	14.4	1.27	14.9
PES-L	12.6	16.2	24.3	8.44	26.3

somewhat cylindrical volume for gas diffusion, which is mainly related to shape and size of permeable gas molecules, while CED can be used as the indicator of interaction of polymer chains and mainly determine the ability in segmental motion of polymer chain.

Packing-inhibited polymers have more unoccupied "free" space and require smaller segmental motions to open up a sufficient passageway for diffusion. Consequently, IMPES-C and IMPES-L tended to have lower cohesive energy densities and exhibited lower diffusion apparent activation energy. On the contrary, the dense chain packing and strong interchain interaction led to PES-Na⁺ and PES-K⁺ reasonably high diffusion apparent activation energy.

For the gas pair to be separated, the E_p of larger penetrant (such as N₂) was usually bigger than that of smaller one (such as H₂ and O₂). As a result, the increase in gas permeability with temperature was always accompanied by a great loss in gas selectivity. As shown in Table 12, the O₂/N₂ selectivity coefficients at 100 °C were found to decrease by about 40% compared to that at 30 °C. It should be noted that, even though the temperature was increased to 100 °C, PES-K⁺ still maintained its high gas selectivity of $\alpha_{\text{H}_2/\text{N}_2}$ in 80.7 and $\alpha_{\text{O}_2/\text{N}_2}$ in 6.90, which were much higher than that of bisphenol A polysulfone (PSF)⁸ at 35 °C. This characteristic is very useful for the gas separation application at high temperature.

Water Vapor Transport Properties. The results of water vapor permeability and its selectivity over N₂ are given in Table 13. These data showed that the free volume and hydrophilicity of polymer were two main

Table 10. Apparent Diffusion Activation Energies and Heats of Solution

polymers	E_D (kJ/mol)				H_s (kJ/mol)			
	O ₂	N ₂	CO ₂	CH ₄	O ₂	N ₂	CO ₂	CH ₄
PES-C	15.9	22.8	21.9	30.5	-3.34	-4.23	-13.2	-9.91
DMPE-C	18.4	26.3	23.1	33.4	-3.31	-2.91	-14.6	-9.23
TMPE-C	13.6	20.2	18.9	27.1	-4.27	-5.64	-14.8	-11.5
IMPE-C	12.8	19.9	18.7	26.3	-4.64	7.32	-16.5	-13.9
IMPE-L	14.6	18.4	18.9	27.5	-5.44	-3.52	-17.5	-13.1
PES-L	22.5	31.9	25.5	43.5	-6.32	-7.56	-17.1	-17.2

Table 11. Gas Permeation, Diffusion Activation Energy, and Solution Heat in PES-L Ionomer Series^a

polymers	O ₂			N ₂		
	E_p	E_D	H_s	E_p	E_D	H_s
PES-L	16.2	22.5	-6.23	24.3	31.9	-7.56
PES-Na ⁺	19.6	24.8	-5.24	27.7	33.3	-5.61
PES-K ⁺	21.5	26.4	-4.88	29.3	36.3	-6.99

^a Unit: kJ/mol.**Table 12. Gas Transport Properties at 100 °C**

polymers	P (barrers) ^a			α		
	H ₂	O ₂	CO ₂	H ₂ /N ₂	O ₂ /N ₂	CO ₂ /CH ₄
PES-C	26.4	2.52	8.41	46.7	4.43	14.5
DMPE-C	23.2	1.98	5.10	48.3	4.12	11.9
TMPE-C	36.0	3.41	10.4	44.8	4.25	13.9
IMPE-C	56.3	7.09	22.3	31.5	3.96	9.87
IMPE-L	88.0	8.96	27.9	38.3	3.90	8.42
PES-L	18.6	1.35	4.47	69.3	5.06	15.1
PES-Na ⁺	14.9	1.21		68.7	6.02	
PES-K ⁺	13.8	1.18		80.7	6.90	

^a P in barrers; 1 barrer = 10^{-10} cm³(STP) cm/(cm² s cmHg).**Table 13. Water Vapor Transport Properties^a**

polymers	P_{N_2}	P_{H_2O}	α_{H_2O/N_2}
PES-C	0.167	3031	18 144
DMPE-C	0.201	2917	14 478
IMPE-L ²²	0.757	5054	6 671
PES-L ²²	0.0437	2840	64 989
PES-Na ⁺ ²²	0.0263	7262	276 121
PES-K ⁺	0.0182	6840	375 824

^a P in barrers; 1 barrer = 10^{-10} cm³(STP) cm/(cm² s cmHg).

factors determining the permeability of water vapor and its separation ability from other gases. The carboxylic groups in PES-L could form hydrogen bonds with water molecules, which was favorable for its water vapor solubility coefficient. However, the dense polymer structure inhibited the water vapor diffusion through PES-L membrane. For PES-L, the latter factor played the dominant role so that the permeability of water vapor in PES-L was slightly lower than that of PES-C. For PES-Na⁺ and PES-K⁺, relative to carboxylic groups, the carboxylate groups had stronger association with water molecule, so that their permeability coefficients of water vapor were about twice as high as that of PES-C. The combination of greatly decreased gas permeability and remarkably increased permeability of water vapor resulted in PES-Na⁺ and PES-K⁺ extremely high selectivity for water vapor over other gases. As shown in Table 13, both of them exhibited H₂O/N₂ selectivity in 10⁵ order of magnitude.

On the other hand, the results in Table 13 revealed that the alkyl substituents were disadvantageous for the water vapor separation from gases because of the hydrophobicity of alkyl groups. The alkyl-substituted polymers in this study generally had increased permeability of gases, which resulted in their low selectivity of H₂O over N₂. For example, compared to PES-C, the

methyl-substituted DMPE-C and isopropyl-substituted IMPE-L had decreased H₂O/N₂ selectivities by 20.2% and 63.2%, respectively.

Conclusion

The polymers in this study can be roughly divided into two categories. One has alkyl substituents on the phenylene rings, such as dimethyl-substituted DMPE-C, tetramethyl-substituted TMPE-C, and diisopropyl-substituted IMPE-C; another includes PES-L, PES-Na⁺, and PES-K⁺, which have strong interchain interaction due to hydrogen bonds or ionic bonds. Different from above polymers, IMPE-L has both bulky isopropyl substituents and carboxylic groups. The systematical variations in chemical structure resulted in great change in physical parameters and so as to considerably affect their gas and water vapor transport properties.

Similar to most of glassy polymers, for the uncondensable O₂/N₂ gas pair, the gas permeability behavior was primarily governed by the diffusivity and diffusivity selectivity, whereas for the CO₂/CH₄ gas pair, the solubility factor exhibited significantly increased contribution to gas permeability and permselectivity. Furthermore, it was favorably found that TMPE-C and IMPE-L displayed both higher permeabilities and higher permselectivities compared to those of the unmodified PES-C.

These polymer membranes showed excellent gas transport properties. Their H₂, O₂, and CO₂ permeability coefficients were in the range 4.89–49.6, 0.2–4.8, and 2.2–25.1 barrers, respectively, while H₂/N₂, O₂/N₂, and CO₂/CH₄ selectivity coefficients were in the range 44–269, 5.4–11.4, and 21–57, respectively. The permeability of water vapor and its selectivity over N₂ in potassium salt form PES-K⁺ were 6840 barrers and 3.8×10^5 , respectively. The wide range of permeability coefficients and permselectivity coefficients provide the possibility to choose some of them for the specific uses such as hydrogen recovery, oxygen enrichment, removal of CO₂ from natural gas as well as the gas dehumidification application.

Acknowledgment. We are grateful to Professor Lianda Jia (Changchun Institute of Chemistry, Chinese Academy of Sciences) for the help of measurements of water vapor and his valuable advice.

References and Notes

- (1) Spillman, R. W. *Chem. Eng. Prog.* **1989**, 85, 41.
- (2) Mazur, W. H.; Chan, M. C. *Chem. Eng. Prog.* **1982**, 78, 38.
- (3) Kresse, I.; Usenko, A.; Springer, J.; Privalko, V. *J. Polym. Sci., Polym. Phys. Ed.* **1999**, 37, 2183.
- (4) Dorkenoo, K. D.; Pfromm, P. H.; Rezac, M. E. *J. Polym. Sci., Polym. Phys. Ed.* **1998**, 36, 797.
- (5) Shigetoshi, M.; Hiroki, S.; Tsutomu, N. *J. Membr. Sci.* **1998**, 141, 21.
- (6) Pixton, M. R.; Paul, D. R. *Macromolecules* **1995**, 28, 8277.

- (7) Chen, T. L.; Yuan, Y. G.; Xu, J. P. Chinese patent 1,038,098, 1988.
- (8) Moe, M. B.; Koros, W. J.; Paul, D. R. *J. Polym. Sci., Polym. Phys. Ed.* **1988**, *26*, 1931.
- (9) Muruganandam, N.; Koros, W. J.; Paul, D. R. *J. Polym. Sci., Polym. Phys. Ed.* **1987**, *25*, 1999.
- (10) Jia, L. D.; Xu, J. P. *Polym. J.* **1991**, *23*, 417.
- (11) Liu, W. Y.; Wang, Z. G.; Chen, T. L.; Xu, J. P. *Proceedings of the 1990 International Membrane and Membrane Processes*, Chicago, IL, 1990; p 836.
- (12) Baeyer, A. *Ann.* **1980**, *202*, 80.
- (13) Wang, Z. G.; Chen, T. L.; Xu, J. P. *J. Macromol. Sci., Pure. Appl. Chem.* **2000**, *A37*, 1571.
- (14) Sugden, S. *J. Chem. Soc.* **1927**, 1786.
- (15) Liu, W. Y.; Chen, T. L.; Xu, J. P. *J. Membr. Sci.* **1990**, *53*, 203.
- (16) Koros, W. J.; Chan, A. H.; Paul, D. R. *J. Membr. Sci.* **1977**, *2*, 165.
- (17) O'Brien, K. C.; Koros, W. J.; Barbari, T. A.; Sanders, E. S. *J. Membr. Sci.* **1986**, *29*, 229.
- (18) Fu, H. Y.; Jia, L. D.; Xu, J. P. *J. Appl. Polym. Sci.* **1994**, *51*, 1405.
- (19) McHattie, J. S.; Koros, W. J.; Paul, D. R. *Polymer* **1991**, *32*, 840.
- (20) Brozoski, B. A.; Painter, P. C.; Coleman, M. M. *Macromolecules* **1984**, *17*, 1591.
- (21) Huang, Y. H.; Cong, G. M.; MacKnight, W. J. *Macromolecules* **1986**, *19*, 2267.
- (22) Xu, J. P.; Wang, Z. G.; Chen, T. L. *ACS Symp. Ser.* **1999**, *733*, 269.
- (23) Breck, D. W. *Zeolite Molecular Sieves*; John Wiley & Sons: New York, 1994; p 636.
- (24) Jeans, J. *An Introduction to the Kinetic Theory of Gases*; Cambridge University Press: London, 1982; p 183.
- (25) Koros, W. J.; Fleming, G. K.; Jordan, S. M.; Kim, T. H.; Hoehn, H. H. *Prog. Polym. Sci.* **1988**, *13*, 339.
- (26) Aitken, C. L.; Koros, W. J.; Paul, D. R. *Macromolecules* **1992**, *25*, 3424.
- (27) Yamamoto, H.; Mi, Y.; Stern, S. A. *J. Polym. Sci., Polym. Phys. Ed.* **1990**, *28*, 2291.
- (28) VanAmerongen, G. J. *Rubber Chem. Technol.* **1964**, *37*, 1065.
- (29) Ghosal, K.; Chern, R. T.; Freeman, B. D.; Daly, W. H.; Negulescu, I. I. *Macromolecules* **1996**, *29*, 4360.
- (30) Fujita, H. *Diffusion in Polymers*; Academic Press: New York, 1968; p 75.
- (31) Lee, W. M. *Polym. Eng. Sci.* **1980**, *20*, 65.
- (32) Maeda, Y.; Paul, D. R. *J. Polym. Sci., Polym. Phys. Ed.* **1987**, *25*, 1005.
- (33) Meares, P. *J. Am. Chem. Soc.* **1954**, *76*, 3415.

MA011185C